Three dimensional metal film catalyst assisted etching of silicon

Wenjun Sheng[1], Tielin Shi[2], Bo Sun[3], Xianhua Tan[4], Ting Jiang[5], Guanglan Liao*[6]

State Key Laboratory of Digital Manufacturing Equipment and Technology, Huazhong University of Science and Technology, Wuhan 430074, China
[1]coraldevil@hust.edu.cn; [2]tlshi@hust.edu.cn; [3]hustsunbo@hust.edu.cn; [4]tanxianhua@hust.edu.cn; [5]jiangting@hust.edu.cn; [6]guanglan.liao@mail.hust.edu.cn

ABSTRACT

Metal assisted chemical etching silicon has emerged as a promising low-cost technology for the fabrication of vertical aligned silicon nanowire arrays. The technology comprises two steps: depositing a layer of 2-D porous siliver film on silicon wafers and then etching in solution. The silicon beneath the silver will be etched continuously along certain crystal orientation so that the silicon nanowire arrays are fabricated. To investigate the influence of the crystal orientation on the etching, we have performed the etching on micro silicon pillar arrays by depositing a layer of 3-D porous siliver film on the surface of the structure. It is found that the etching behavior is related not only to the crystal orientation of the silicon substrate but also to the shape of the 3-D siliver film. This etching behavior can be developed further for the fabrication of 3-D silicon structure.

Keywords: Etching, silicon nanowire, catalyst

1 INTRODUCTION

Applications of silicon nanowires are becoming widespread across a variety of tecnology fields recently. Many kinds of devices base on silicon nanowires such as solar cells [1,2], lithium ion batterys [3], biochemical sensors [4] are developed. Integration of silicon nanowires can improve the device performance remarkablely [5, 6]. There are a lot of methods for the fabrication of silicon nanowires such as VLS (vapor-liquid-solid) growth [7], RIE (Reactive ion etching) [8], etc. Metal assisted chemical etching (MACE) is a promising low-cost method emerging recently [9-11]. The fabrication of silicon nanowires is based on anisotropic etching depending on crystal orientation [12]. Traditionally, the etching is conducted on flat silicon substrate with 2-D silver film as catalyst to fabricate aligned silicon nanowires [13, 14]. To investigate the anisotropic characteristic of this method, we design contrast experiments, i.e. etching conducted on silicon pillars with 3-D metal film catalyst and flat silicon substrates with 2-D metal film catalyst.

2 EXPERIMENTAL PROCEDURES

In the experiments, P-type, boron-doped, 1-10 Ω•cm Si(100) wafers were used. All the etching was performed in teflon vessels under room temperature.

Silicon wafers were cut into 10mm^2 pieces and then ultrasonically cleaned with acetone and ethanol for 10 min, respectively. Photolithography was performed with AZ5214 photoresist on the samples to define the pattern of hexagonally distributed circles with 25μm in diameter and 50μm in pitch. Silicon pillars were fabricated with inductively coupled plasma reactive ion etching (ICP-RIE) using the photoresist patterns. During the ICP-RIE, bosch process was used with the process gas SF_6 and C_4F_8. Then the samples were washed with piranha solution of H_2SO_4/H_2O_2 (3:1) at 120 ℃ for 10 min, so as to remove organic remains generated during ICP-RIE.

To perform the MACE, flat silicon pieces or silicon pieces with pillars were immersed into RCA solution of $NH_4OH/H_2O_2/H_2O$ (1: 1: 5) for 10 min at 70 ℃ and washed with excess deionized water. Then the samples were put into a solution containing 5.0M HF and 0.01M $AgNO_3$ for 1 min to deposit a layer of silver film. Here the siliver film is deposited by galvanic displacement reaction on the suface of the samples [15]. After that, the samples were put into the etching solution of 5.0M HF and 0.5M H_2O_2 for 5 min. Finally, the samples were washed using concentrated nitric acid to remove the residual siliver catalyst.

The morphology of the fabricated nanostructures was characterized with scanning electron microscopy (SEM). A single silicon nanowire was characterized using transmission electron microscope (TEM). X-ray diffraction (XRD) was utilized to analysis the single-crystal structure of the silicon nanowires.

3 RESULTS AND DISCUSSIONS

3.1 mechanism

The morphology of the siliver film deposited on the flat (100) silicon substrate is characterized with SEM as shown in Fig.1(a). It can be seen that the silver film is porous. During the etching, half-cell reactions that include cathode and anode reactions happen [16]. The reactions are described as follows:

(1) Cathode:
$H_2O_2 + 2H^+ + 2e^- \rightarrow 2H_2O$
(2) Anode:
$Si + 2H_2O \rightarrow SiO_2 + 4H^+ + 4e^-$

$SiO_2+6HF \rightarrow H_2SiF_6+2H_2O$

$Si+6HF \rightarrow H_2SiF_6+4H^++4e^-$

(3) Overall:

$Si+2H_2O_2+6HF \rightarrow H_2SiF_6+4H_2O$

As mentioned above, the side of the silver film facing the etching solution acts as the cathode, which catalyzes H_2O_2 reduction and consums H^+ and electrons. The other side of the silver film facing the silicon acts as the anode which catalyzes the silicon oxidation and generates H^+ and electrons. The produced SiO_2 is corroded into H_2SiF_6 by HF and dissolves in the soluton. These processes proceed continually so that the silicon nanowires form.

3.2 MACE on flat substrate

The morphology of the fabricated silicon nanowires on flat (100) silicon substrate is shown in Fig.1(b) and (c). Fig.1(b) is the side view of the silicon nanowires. It can be found that the etching direction is perpendicular to the surface of the silicon substrate and the nanowires are vertical aligned to the substrate. Fig.1 (c) is the the top view of the silicon nanowires. This implies that the silver film moves along (100) crystal orientation during the MACE. The TEM picture of a single silicon wire is shown in Fig.2. Fig. 2(a) is the low resolution picture of a silicon nanowire with the diameter less than 100 nm. Fig.2(b) is the high resolution picture of the silicon nanowire, implying that the axis direction is the (100) crystal orientation. Fig.2(c) shows the XRD pattern of the as-prepared silicon nanowires on planar silicon before removing the silver catalyst. The diffraction peaks at 44.3°, 64.4° and 81.5° belong to the crystalline orientation (200), (220) and (222) of the Ag catalyst, respectively. The diffraction peak of silicon corresponding to (311) is observed from the pattern. This indicates that the obtained silicon nanowires are uniform and highly oriented to the silicon wafer, consistent with the SEM results. For the (111) and (110) silicon substrates, the etching is along (111) and (100) crystal orientation [12] so that the nanowires is slanted to the surface of the (110) silicon substrate and vertical to (111) silicon substrate, respectively. Therefore, the etcing on silicon flat substrate shows an obvious anisotropic characteristic depending on the crystal orientation.

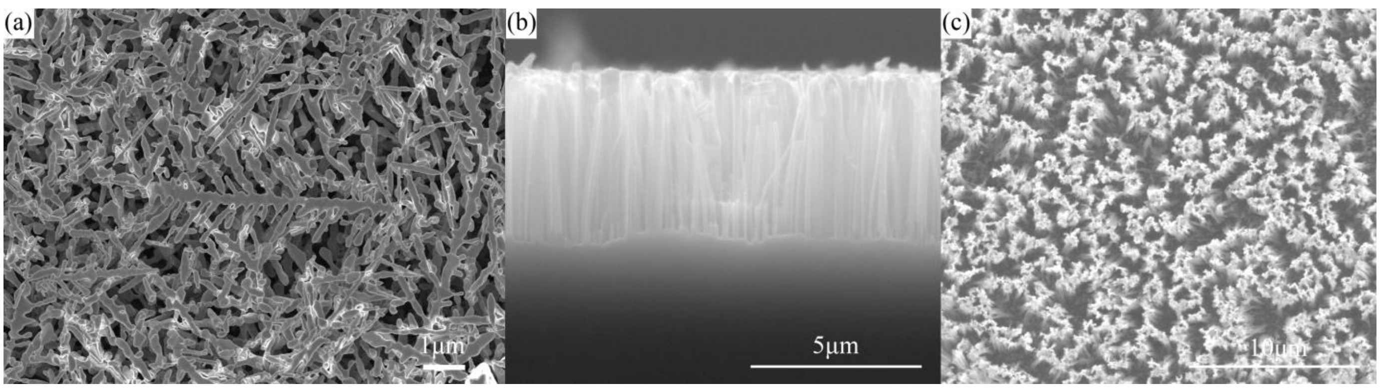

Fig.1 (a) The morphology of the silver film. (b), (c) The top and side view of the silicon nanowire arrays.

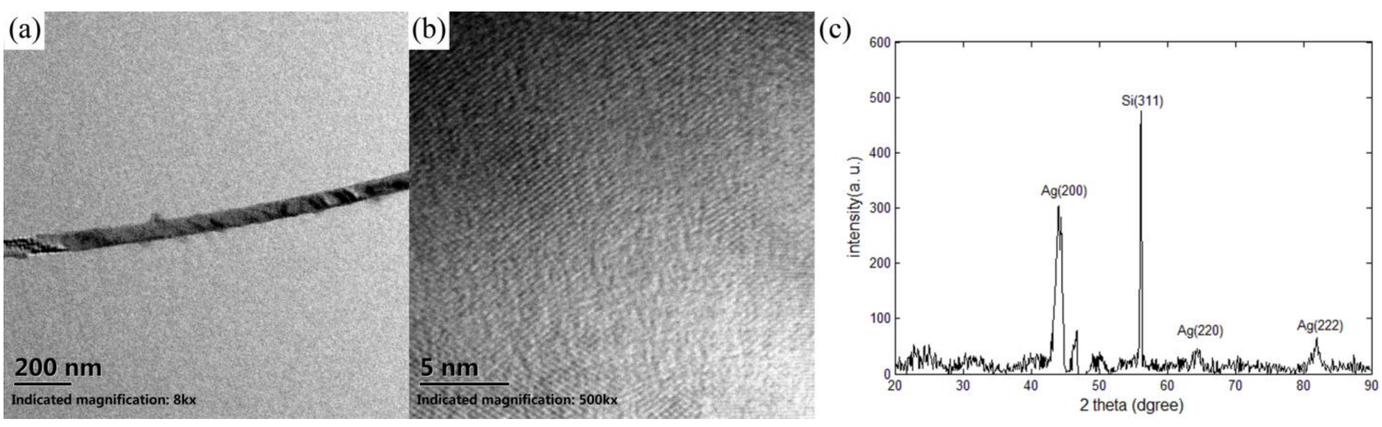

Fig.2 (a), (b) low and high resolution TEM pictures of the silicon nanowire. (c) The X-ray diffraction (XRD) pattern of the silicon nanowires with Ag catalyst.

3.3 MACE on silicon pillars

To investigate the influence of the crystal orientation to the etching, we perform the MACE on silicon pillars

NSTI-Nanotech 2013, www.nsti.org, ISBN 978-1-4822-0584-8 Vol. 2, 2013

fabricated on (100) silicon substrate. Obviously, (100) crystal orientation is perpendicular to the top surface and the bottom of the pillars. On the side of the pillars, all the crystal orientations are exposed. The deposited silver film are cylindrical, the same as the pillars. After the etching, the top of the silicon pillars is covered with nanowires which are vertical aligned to the top surface of the pillars, as shown in Fig.3(a) and 3(d). The side of the pillars is also covered with silicon nanowires as shown in Fig.3(b) and 3(e). It can be seen that the silicon nanowires are a little bend and turn shorter gradually when close to the bottom of the silicon pillars. At the root of the pillars, the nanowires almost disappear. Fig.3(c) and 3(f) display the excessive etching results, which is a flower-like structure. There are some nanowires at the top of the pillars and some slant etching traces around the nanowires. Many nanoholes can be found on the bottom of the pillars.

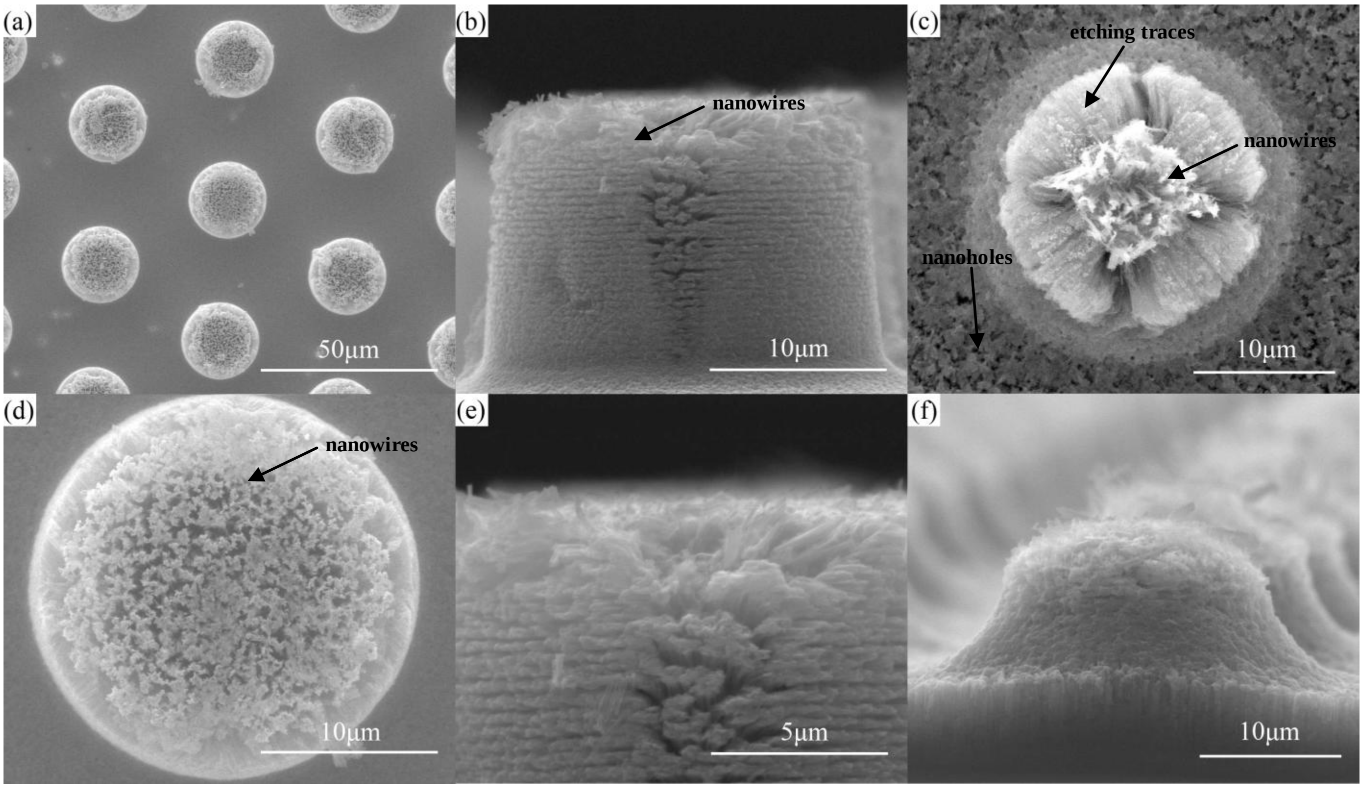

Fig.3 (a), (d) and (b), (e) are the top and side view of the pillars with nanowires. (c), (f) are the excessive etching results.

The etching process is hypothesized as shown schematically in Fig. 4. The silver film is supposed to be a whole. There may be some kind of electrochemical force making the catalyst moving towards the contacted silicon and catalyzing the etching of the silicon. During the MACE, the silver film on the silicon pillars moves or even deforms to make the etching proceed. The shape of the 3D porous silver film attached to the pillars is shown in Fig. 4. Obviously, the shape of the silver film is the same as the pillars. When the substrate with pillars is immersed into the solution, the etching reactions happen and the MACE begins. The siliver film etches towards the contacted silicon. On the side surface of the pillars, all crystal orientations are exposed. So the etching can not proceed along some preferred crystal orientation. On the top of the pillars, the silver film can etch along the preferred (100) crystal orientation. On the bottom of the pillars the film should have etched the silicon along (100) crystal orientation. Because of the adhesion of the siliver film to the side of the pillars, the silver film on the bottom can not move downwards and the etching can not proceed. To make the etching proceed, the only possible movement of the siliver film is rotating towards the core of pillars along the root of the pillars. As a result, the nanowires on the side of the pillars forms in different length. Here the etcing is not related to the crystal orientation but the 3-D movement of the silver film. When the etching is excessive, the silver film on the bottom of the pillars is broken into particles because of the stress generated during the etching. Thus, a lot of nanoholes are generated at the bottom of the pillars catalized by the silver particles, as shown in Fig 3(c). On the side of the pillars, the fabricated silicon nanowires are etched away because of the deforming the silver film, and some etching traces are left around the silicon nanowires, as shown in Fig.3(c).

Therefore, the etching behavior is different to the traditional etching process only depending on crystal orientation. The shape and the movement of the siliver film affect the etching process greatly. These results indicate that not only the crystal orientation but also the silver film shape will affect the etching behavior in MACE. The restriction of the crystal orientation may be avoided. This phenomenon may be used for 3D fabrication if controlling the movement of the silver film. This will promote the application of MACE greatly. Also, the fabricated hierarchical structure with silicon micro pillars and nanowires may provide potential application in microfluid [17], bioMems [18,19], solar cells [20], etc.

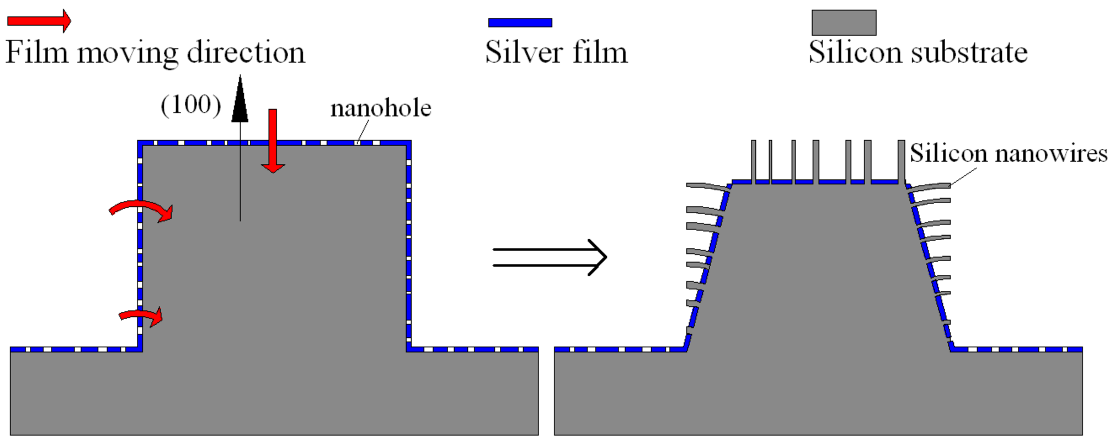

Fig.4 The movement of the sliver fim.

4 CONCLUSIONS

In this work, MACE is performed on flat silicon substrates with 2-D silver film as catalyst and silicon pillars with 3-D silver film as catalyst. The etching behavior of 3-D silver film is different to the traditional etching only depending on the crystal orientation. This phenomenon can be used for 3-D fabrication which will be studied further. The fabricated hierarchical silicon structure may provide potential application in microfluid [17], bioMems [18,19], solar cells [20] and so on.

ACKNOWLEDGEMENTS

The authors thank the Huazhong University of Science & Technology Analytical and Testing Center for the help of XRD characterization. The authors are grateful for the financial supports by National Key Basic Research Special Fund of China (Grant No. 2009CB724204) and National Natural Science Foundation of China (Grant Nos. 51175210 and 51222508).

REFERENCES

[1] Bozhi Tian, Xiaolin Zheng, Thomas J. Kempa, et.al. Nature, 449, 885-889, 2007
[2] L. Tsakalakos, J. Balch, J. Fronheiser, et.al. Appl. Phys. Lett. 91, 233117, 2007
[3] Candace K. Chan, Hailin Peng, Gao Liu, et.al. Nature Nanotechnology, 3, 31-35, 2008
[4] Dong Rip Kim, Chi Hwan Lee and Xiaolin Zheng, Nano Lett., 9 (5), 1984-1988, 2009
[5] Erik Garnett and Peidong Yang, Nano Lett., 10 (3), 1082-1087, 2010
[6] Fangxia Shen, Jindong Wang, Zhenqiang Xu, et.al. Nano Lett., 12 (7), 3722-3730, 2012
[7] J. B. Hannon, S. Kodambaka, F. M. Ross, et.al. Nature, 440, 69-71, 2006
[8] Z. Huang, H. Fang, J. Zhu, et.al. Advanced Materials, 19 (5), 744-748, 2007
[9] Rykaczewski K, Hildreth OJ, Wong CP, et.al. Nano Lett., 11 (6), 2369-2374, 2011
[10] Winston Chern, Keng Hsu, lk Su Chun, et.al. Nano Lett., 10 (5), 1582-1588, 2010
[11] Ke Sun, Yi Jing, Namseok Park, et.al, J. Am. Chem. Soc., 132 (44), 15465-15467, 2010
[12] Kuiqing Peng, Aijiang Lu, Ruiqin Zhang, et.al, Advanced Functional Materials, 18 (19), 3026-3035, 9, 2008
[13] Kuiqing Peng, Ying Xu, Yin Wu, et.al. Small, 1 (11), 1062-1067, 2005
[14] Ming-Liang Zhang, Kui-Qing Peng, Xia Fan, et.al. J. Phys. Chem. C, 112 (12), 4444-4450, 2008
[15] Peng K, Fang H, Hu J, et.al. 16(3), 387-394, 2006
[16] K. Peng, Y. Yan, S. Gao, Advanced Functional Materials, 13 (2), 127-132, 2003
[17] Sunitha Nagrath, Lecia V. Sequist, Shyamala Maheswaran, Nature, 450, 1235-1239, 2007
[18] Shutao Wang, Hao Wang, Jing Jiao, et.al. 121 (47), 9132-9135, 2009
[19] Shutao Wang, Hao Wang, Jing Jiao, et.al. Angewandte Chemie International Edition, 48 (47), 8970-8973, 2009
[20] Jian Shi, Yukihiro Hara, Chengliang Sun, et.al. Nano Lett., 11 (8), 3413-3419, 2011